

# Magneto-driven Shock Waves in Core-Collapse Supernova

Tomoya Takiwaki<sup>1</sup>, Kei Kotake<sup>1</sup>, Shigehiro Nagataki<sup>2</sup>, and Katsuhiko Sato<sup>1,3</sup>

<sup>1</sup>*Department of Physics, School of Science, the University of Tokyo, 7-3-1 Hongo, Bunkyo-ku, Tokyo 113-0033, Japan*

<sup>2</sup>*Yukawa Institute for Theoretical Physics, Kyoto University, Kyoto 606-8502, Japan*

<sup>3</sup>*Research Center for the Early Universe, School of Science, the University of Tokyo, 7-3-1 Hongo, Bunkyo-ku, Tokyo 113-0033, Japan*

takiwaki@utap.phys.s.u-tokyo.ac.jp

## ABSTRACT

We perform a series of two-dimensional magnetohydrodynamic simulations of the rotational core-collapse of a magnetized massive star. We employ a realistic equation of state and take into account the neutrino cooling by the so-called leakage scheme. In this study we systematically investigate how the strong magnetic field and the rapid rotation affect the propagation of the shock waves. Our results show that in the case of the strong initial poloidal magnetic field, the toroidal magnetic field amplified by the differential rotation, becomes strong enough to generate a tightly collimated shock wave along the rotational axis. On the other hand, in the case of the weak initial magnetic field, although the differential rotation amplifies toroidal magnetic field over the long rotational period, the launched shock wave is weak and the shape of it becomes wider. The former case is expected to be accompanied by the formation of the so-called magnetar. Our models with rapid rotation and strong magnetic field can create a nozzle formed by the collimated shock wave. This might be the analogous situation of the collapsar that is plausible for the central engine of the Gamma-Ray Bursts.

*Subject headings:* supernovae: collapse, rotation — magnetars: pulsars, magnetic field — methods: numerical — MHD — gamma rays: bursts

## 1. Introduction

The study of collapse driven supernovae is important not only for itself but also for the understanding of other process of astrophysical relevance, such as nucleosynthesis of heavy

elements and chemical evolutions in the universe (e.g., Arnett 1996), radiation of neutrinos in the universe (Raffelt 2002), the gravitational waves (Andersson 2003), and possibly gamma-ray bursts (GRB) and hypernovae (MacFadyen & Woosley 1999). In spite of its importance and extensive investigations done so far, the explosion mechanism has not been clarified yet.

Except for the special cases, the shock wave generated by the core bounce stalls and becomes an accreting shock in the core. Although neutrino heating are expected to revive the shock wave and lead to the successful explosion (Wilson 1985), recent theoretical studies that elaborate the neutrino transport method and detailed microphysics and/or general relativity, failed to produce explosions (Rampp & Janka 2000; Liebendörfer, Mezzacappa, & Thielemann 2001; Thompson, Burrows, & Pinto 2003; Buras, Rampp, Janka, & Kifonidis 2003). However, it should be noted that most of them assume spherical symmetry (see, however, Buras et al. 2003).

On the other hand, there are convincing observations, which require the revision of the spherically symmetric stellar collapse. Rather common correlation between the asymmetry and the collapse-driven supernovae has been reported by the observation of the polarization (Wang et al. 2002). It is also well known that SN 1987A is globally asymmetric (Cropper et al. 1988; Papaliolis et al. 1989), which is directly confirmed by the images of the *Hubble Space Telescope* (Plait, Lundqvist, Chevalier, & Kirshner 1995). The observed light curve also supports jet-like explosion (Nagataki, Hashimoto, Sato, & Yamada 1997; Nagataki 2000). The asymmetry is likely to have originated from the core dynamics (Khokhlov et al. 1999). Provided the facts that the progenitors of the collapse-driven supernovae are a rapid rotator on the main sequence (Tassoul 1978) and that the recent theoretical studies suggest a fast rotating core prior to the collapse, it is important to incorporate rotations in simulations of core collapse (Heger, Langer, & Woosley 2000).

In addition, after the discovery of pulsars, it was reasonable to explore the issue of whether or not the rotation and magnetic fields associated with pulsars could be a significant factor in the explosion mechanism. So far there have been some works devoted to the understanding of the effect of rotation and magnetic field on the supernova explosion mechanism (Leblanc & Wilson 1970; Mueller & Hillebrandt 1981; Bodenheimer & Woosley 1983; Symbalisty 1984; Mönchmeyer et al. 1989; Yamada & Sato 1994; Fryer & Heger 2000; Kotake, Yamada, & Sato 2003). The magnetocentrifugal jets generated by the strong toroidal magnetic fields in stellar collapse may explain why all core collapse supernovae are found to be substantially asymmetric and predominantly bipolar (Wheeler, Meier, & Wilson 2002). With the typical dipole fields of  $10^{12}\text{G}$  and rotation periods of several tens of milliseconds, however implying electro dynamic power of only  $\approx 10^{44} - 10^{45}\text{ergs}^{-1}$ , a strong robust explosion seemed unlikely. Several factors, such as observation of magnetar (Duncan & Thomp-

son 1992), may lead to a need to reexamine the conclusion. For analyzing the origin of the strong magnetic field, it is necessary to investigate the magnetohydrodynamic processes such as magnetorotational instability (MRI) and the field line wrapping mechanism (Ostriker & Gunn 1971; Bisnovatyi-Kogan 1971; Bisnovatyi-Kogan & Ruzmaikin 1976; Kundt 1976; Balbus & Hawley 1998; e.g. Meier, Epstein, Arnett, & Schramm 1976; Akiyama, Wheeler, Meier, & Lichtenstadt 2003). These processes strongly depend on the configuration and the strength of the magnetic fields. We think that it's still worth investigating the model of strong magnetic field and rapid rotation those have not been considered sufficiently so far. It should be mentioned that such models may be related to some theoretical models of GRBs and magnetar (Proga, MacFadyen, Armitage, & Begelman 2003; Lyutikov, Pariev, & Blandford 2003). By changing the strength of rotation and the poloidal magnetic fields in a parametric manner, we investigate how the rapid rotation and the strong magnetic fields affect the property of the shock waves and the explosion energy. By so doing, we hope to understand the difference of the hydrodynamic behaviors between our models and the models for the canonical supernovae discussed so far.

We describe the numerical method and the initial model in the next section. In the third section, we show the numerical results. The summary and some discussions are given in the last section.

## 2. Method of Calculation

### 2.1. Basic Equations

The numerical method for magnetohydrodynamic (MHD) computations employed in this paper is based on the ZEUS-2D code (Stone, Mihalas, & Norman 1992). The basic equations for the evolution are written as follows,

$$\frac{D\rho}{Dt} + \rho\nabla \cdot \mathbf{v} = 0, \quad (1)$$

$$\rho \frac{D\mathbf{v}}{Dt} = -\nabla P - \rho\nabla\Phi + \frac{1}{4\pi} (\nabla \times \mathbf{B}) \times \mathbf{B}, \quad (2)$$

$$\rho \frac{D}{Dt} \left( \frac{e}{\rho} \right) = -P\nabla \cdot \mathbf{v} - L_\nu, \quad (3)$$

$$\frac{\partial \mathbf{B}}{\partial t} = \nabla \times (\mathbf{v} \times \mathbf{B}), \quad (4)$$

$$\Delta\Phi = 4\pi G\rho, \quad (5)$$

where  $\rho, P, \mathbf{v}, e, \Phi, \mathbf{B}, L_\nu$  are the mass density, the gas pressure including the radiation pressure from neutrino's, the fluid velocity, the internal energy density, the gravitational potential, the magnetic field and the neutrino cooling rate, respectively. We denote Lagrange derivative, as  $\frac{D}{Dt}$ . The ZEUS-2D is an Eulerian code based on the finite-difference method and employs an artificial viscosity of von Neumann and Richtmyer to capture shocks. The time evolution of magnetic field is solved by induction equation, Eq. (4). In so doing, the code utilizes the so-called constrained transport (CT) method, which ensures the divergence free ( $\nabla \cdot \mathbf{B} = 0$ ) of the numerically evolved magnetic fields at all times. Furthermore, the method of characteristics (MOC) is implemented to propagate accurately all modes of MHD waves. The self-gravity is managed by solving the Poisson equation with the incomplete Cholesky decomposition conjugate gradient (ICCG) method. In all the computations, spherical coordinates are used. We made several major changes to the base code to include the microphysics. First we added an equation for electron fraction to treat electron captures and neutrino transport by the so-called leakage scheme (Epstein & Pethick 1981). The cooling rate,  $L_\nu$ , is also estimated by the scheme. For a more detailed description of this scheme, see Kotake 2003 (Kotake, Yamada, & Sato 2003). Second we have incorporated the tabulated equation of state (EOS) based on relativistic mean field theory instead of the ideal gas EOS assumed in the original code (Shen et. al. 1998).

## 2.2. Initial Models

We make precollapse models by taking the profile of density, internal energy, electron fraction distribution from  $20M_\odot$  rotating presupernova model of Heger (Heger, Langer, & Woosley 2000), and assume the profile of rotation and the magnetic field as follows. As for the rotation profile, we assume the cylindrical rotation:

$$\Omega(X, Z) = \Omega_0 \frac{X_0^2}{X^2 + X_0^2} \frac{Z_0^4}{Z^4 + Z_0^4}, \quad (6)$$

where  $X$  and  $Z$  denote distance from rotational axis and the equatorial plane. We adopt the value of parameters,  $X_0$  and  $Z_0$ , as  $10^7\text{cm}$ ,  $10^8\text{cm}$ , respectively. We assume that the initial magnetic field is uniform and parallel to the rotational axis:

$$B_z = B_0. \quad (7)$$

Although recent stellar evolution studies show that toroidal magnetic field components may be stronger than the poloidal ones prior to the collapse (Spruit 2002), uncertainty remains still in the model. In this study we choose the poloidal magnetic fields in order to see the mechanism of field amplification (Wheeler, Meier, & Wilson 2002). We compute 12 models

changing the total angular momentum and strength of magnetic field by varying the value of  $\Omega_0$  and  $B_0$ . The model parameters are given in Table 1. The models are named after this combination, with the first letters, B12, B10.5, B9, B0, representing strength of initial magnetic field, the following letter, TW1, TW2, TW4 representing the initial  $T/|W|$ . Here  $T/|W|$  indicates the ratio of rotational energy to absolute value of gravitational energy.

### 3. Numerical Results

#### 3.1. The Hydrodynamic Features

We will first summarize some important magnetohydrodynamic aspects which are common to our models. The time evolution of our models can be specified by the three stages. The first stage is between the onset of the core collapse and the core bounce. The matter falls to the center of the core everywhere. Therefore the magnetic fields frozen into the matter are compressed in this stage. Next we call the epoch from the core bounce to the propagation of the shock waves as the second stage. Since the rotation prevents the matter from infalling around the equatorial plane, the matter near the rotational axis falls more quickly. The core bounce first occurs near the axis. High entropy regions are generated near the rotational axis, and they begin to propagate along the axis. The toroidal magnetic field is produced by the MHD processes in the shock wave. The amplification of the magnetic fields is discussed elaborately in subsection 3.2. After the second stage, the shock wave is generated and propagates outward. We call this stage as the third stage. The properties of the shock waves are different among the models, however it is common that the toroidal magnetic field is transferred by the shock, see the top panels of Figure 1. Especially in the models of the moderate magnetic field such as B10.5TW1, B10.5TW2 and B10.5TW4, we found unique hydrodynamical features. The shock wave tends to stall in these models. After the stall the hydrodynamical features resemble to those in the second stage. The matter falls easily near the rotational axis, and the weaker shock wave is generated by the difference of the magnetic and the matter pressures between inside and outside of the shock wave. After the launch of the shock the epoch goes to the third epoch. The second stage and the third stage are repeated. The arguments of specific behaviors among models are starting in the following.

We show the differences of each model in the three stages mentioned above. Some of the final profiles are presented in Figure 2. It can be clearly seen in the figure that there is a variety of final state of shocks. We investigate the origin of this variety in the following. Since the rotation does not affect qualitative features in our computation so much, we mainly focus on the hydrodynamic features of each models caused by the initial strength of the magnetic

field.

In the strong magnetic models such as B12TW1, B12TW2, and B12TW4, tightly collimated jet-like shock waves are found at the third stage. Strong hoop stress is produced by the field wrapping at the launch of the shock wave. The launched shock waves are pushed by the strong magnetic pressure, and propagate along the rotational axis, while keeping its shape collimated. The discussion for the collimation is given in the last of section 3.2. The matter around the polar axis is expelled by the collimated jet-like shock waves. These dynamic behaviors are seen in Figure 1 in the case of B12TW4. In all stages there are no qualitative differences among these three models, such as shape of the jet and the remaining configuration of the matter. A major quantitative difference is the explosion energy discussed in section 3.3.

On the other hand, the shock waves become less collimated near the rotational axis in the weak magnetic models such as B9TW4, B9TW2, B9TW1, B0TW4, B0TW2 and B0TW1. The prolate shock waves at the core bounce become rather spherical after the shock stalls. This is caused by the magnetic and the matter pressure. The difference among them is seen at a later stage rather. In the case of the weak rotation, the shock front revived by the magnetic and the matter pressure propagates rather spherically. On the other hand, in the case of the strong rotation the magnetic pressure produced by the field wrapping pushes the matter along the rotational axis at the launch of the shock. However this weak prolate shock wave becomes spherical soon due to weak hoop stress.

In the case of the moderate magnetic fields such as B10.5TW4 and B10.5TW2, the evolutions of the shock waves are rather complicated, see the right panels of Figure 3. In these cases, jet-like shock waves are launched along polar axis, and stall very soon. 20ms after the shock-stall, the shock wave is found to be revived due to the magnetic and the matter pressure and propagates along the rotational axis again (right top). However in this case, the hoop stress is not strong enough to keep the collimation of the prolate shock wave (right middle). Then the prolate shock wave becomes spherical. The shock front propagates repeating these behaviors (right bottom), the shape of shock wave becomes spherical in the end. On the other hand, in the case of B10.5TW1 (see the left panels of Figure 3), the stalled jet-like shock waves launched along polar axis are revived by the matter pressure (left top). The weak rotation makes the second bounce robust as the weak rotation makes first bounce robust. The jet-like shock propagates along the rotational axis strongly (left middle). After the shock propagates along rotational axis, this robust shock wave becomes wider (left bottom). The strength of the rotation rate makes these differences, i.e. in the case of weak rotational model, the strong shock wave is generated. This shock front propagates before the matter behind the shock wave expands. In the rapid rotating model the weak

shock waves is likely to stall and expand due to the matter and magnetic pressures. For the analysis of these behaviors, we focus on the value of plasma beta which is ratio of the gas pressure to the magnetic pressure in the following section.

### 3.2. Behavior of Magnetic Field and Degree of Collimation

We explain how the magnetic fields affect the propagation of the shock waves in this subsection. First we briefly explain two MHD processes so-called magnetorotational instability (MRI) and field wrapping. We focus on one of the MRI of the vertical component of the magnetic field, because in our simulation initial magnetic field is vertical. It is noted that this MRI produces the  $X$  component of the magnetic field. This MRI is important because the onset of the MRI requires the differential rotation of the core, i.e.  $\frac{d\Omega}{dX} < 0$ , which is globally content in the stellar collapse. The time-scale of the maximum growth of the instability is evaluated as  $\tau_{\text{MRI}} = 4\pi \left| X \frac{\partial \Omega}{\partial X} \right|^{-1}$  (Balbus & Hawley 1998). If this value is constant, the MRI process amplifies the  $X$  component of the magnetic field exponentially. As for the field wrapping, it winds up poloidal magnetic field along axis, and generate toroidal magnetic field. This process also requires the differential rotation. It's characteristic time scale is  $\tau_{\text{WRAP}} = 4\pi \left| \frac{\partial B_\phi}{\partial t} \right|^{-1} = 4\pi \left| \frac{B_X}{B_\phi} \left( X \frac{\partial \Omega}{\partial X} \right) + \frac{B_Z}{B_\phi} \left( X \frac{\partial \Omega}{\partial Z} \right) \right|^{-1}$  which is derived from induction equation (e.g. Meier, Epstein, Arnett, & Schramm 1976). The definition of  $\tau_{\text{WRAP}}$  shows that  $\tau_{\text{WRAP}}$  becomes short if the poloidal magnetic field dominates toroidal component. It means that MRI can increase the seed poloidal component of magnetic field which amplifies the toroidal magnetic field due to the field wrapping. It should be noted that since our simulation assumes axisymmetry, the poloidal component can not be produced from the instability of the toroidal component.

We show how magnetic fields are amplified in each stage by comparing the growth time-scale of MRI and field wrapping (see Figure 4). In the first stage, the typical time-scale for this stage is less than 200ms after the onset of the gravitational collapse. Although the initial magnetic fields are parallel to the rotational axis, the  $X$  component is found to be formed by the infall of the matter. See the left top panel of Figure 4, the minimum values of  $\tau_{\text{MRI}}$  at this stage is about 300ms. Since the time-scale is much longer than the dynamical time-scale, thus the  $Z$  component of magnetic field is changed to the  $X$  component mainly due to the compression by the infalling material. Since  $\tau_{\text{WRAP}}$  is very short, the toroidal component of the magnetic field is rapidly amplified. In the second stage, we found that the toroidal magnetic field produced by the field wrapping becomes to dominate over the poloidal component in the central region. Since the flow in this region is complicated by the convective flow, the magnetic fields frozen into the flow become also complicated. These

convections produce the  $X$  component of the magnetic field from the initial  $Z$  component. In this stage, the MRI can grow in the center of core. See the left middle panel of Figure 4, the characteristic time scale of instability is about 10ms at the center of the core. Thus, MRI is likely to generate the  $X$  component from the  $Z$  component. It is also seen the middle right panel in Figure 4 that the time-scale of the wrapping is found to be shorter than that of the MRI. Therefore the toroidal magnetic field is predominantly generated by the wrapping in this stage. In the third stage, since the toroidal magnetic field dominates over the poloidal magnetic field behind the shock wave, the wrapping time scale becomes very long. In this era the main process of field amplification is the MRI. This means that toroidal magnetic field is not dominantly generated by the field wrapping. This strong magnetic field is transferred by the propagation of the shock wave.

Here it should be mentioned about the amplification of the magnetic field in the case of the weak initial magnetic field. Even if initial magnetic field is weak, long-time rotation increases strength of magnetic field. In this era dominant process of field amplification is MRI. We found the interesting example of these effects in our simulation. The differential rotation amplifies strong toroidal magnetic field even if the initial magnetic field is weak, see Figure 5. Consequently the small weak jet pushed by the magnetic pressure is generated as seen in Figure 5. This situation occurs in the only later stage (366ms from core bounce) because it takes long time to wind up the toroidal magnetic field if the initial poloidal magnetic field is weak.

Finally we explain the magnetic effect on the collimated shock wave. First we show plasma  $\beta$  which is the ratio of the magnetic pressure,  $P_{\mathbf{B}} = \frac{\mathbf{B}\cdot\mathbf{B}}{8\pi}$  to the gas pressure,  $P$  in the top panel of Figure 6. This figure shows the region where the magnetic field predominantly affects the dynamics of the matter. We can see jet is broaden if  $\beta > 1$  in the interior of the shock waves. However this is not enough to discuss the dynamical role of the magnetic field, because the magnetic fields have two aspects for the collimation. The hoop stress,  $\frac{B_{\phi}^2}{X}$ , collimate shock wave, however the gradient of the magnetic pressure,  $\frac{1}{2}\frac{\partial B_{\phi}^2}{\partial X}$ , expand shock wave. Therefore we show the ratio of the hoop stress to the gradient of the magnetic pressure in the bottom panel of Figure 6. This figure demonstrates that the hoop stress work near the rotational axis and even if the case of the collimated shock wave magnetic pressure is dominant at the shock front. It means that even the collimated shock wave tend to expand parallel to the  $X$  axis. Therefore the degree of the collimation is not determined by the magnetic field only. The velocity of the shock front is another factor which governs the degree of the collimation. In the Figure 6, left panels are of B12TW2 and right panels are of B10.5TW1. In B12TW2 the  $Z$  component of the velocity of the shock front near the rotational axis at the launch is  $4.0 \times 10^9$ cm/s on the contrary, that of B10.5TW1 is  $1.5 \times 10^9$ cm/s. This figure shows that the high  $Z$  component of the velocity can make the

shock front propagates before it expand to  $X$  direction. Such a strong collimated shock wave tends to propagate entirely through iron core. On the other hand, the weak widely expanding jet or prolate shock wave tends to stall.

### 3.3. The Explosion Energy

In this subsection, we discuss the relation between the explosion energy and the initial strength of the magnetic field and the rotation. We define the explosion energy as,

$$E_{\text{explosion}} = \int_{\text{D}} dV \left( \frac{1}{2} \rho \mathbf{v} \cdot \mathbf{v} - \rho \Phi + e + \frac{1}{8\pi} \mathbf{B} \cdot \mathbf{B} \right). \quad (8)$$

Integrating region, D, represents the domain where the integrand is positive. This quantity is evaluated when shock wave arrives at the radius of 1500km at the  $Z$  axis. We use this quantity as the measure of the strength of the explosion.

The explosion energy for each model is summarized in Table 2. There is a general tendency that the rapid rotation decreases the explosion energy. The centrifugal force prevents the matter near the equatorial plane from falling rapidly, therefore bounce occurs weakly. It is consistent to the previous work (Yamada & Sato 1994; Yamada & Sawai 2004). Further more it's found that the explosion energy monotonically increases with the initial magnetic field strength. The magnetic pressure plays an important role in the explosion. The strong toroidal magnetic field collimates the shock wave. Thus it requires relatively low energy for shock wave to expel the matter near the rotational axis. As a result, the strong magnetic field is favorable to the robust explosion in the limited region. On the other hand, the weak magnetic fields does not deviate the dynamics from pure rotation case until the core bounce. However it's found that they affect the dynamics in the later phase. In fact, the model, which does not explode without magnetic fields, explodes as a result of the field amplification.

To summarize, we find that the slow rotation and the strong magnetic field increase the explosion energy, and that the even weak magnetic fields can contribute to the explosion at the later stage.

## 4. Summary and Discussion

We have done a series of two-dimensional magnetohydrodynamic simulations of the rotational core collapse of a magnetized massive star. In this study, we have systematically investigated how the strong magnetic fields and the rapid rotation affect the dynamics from

the onset of the core-collapse to the shock propagation in the iron core. By analyzing the properties of the shock waves and estimating the explosion energies, we have obtained the results in the following.

1. The explosion energy decreases with the initial rotation rates, on the other hand, increases with the initial strength of the magnetic fields. As a result, it is found that the combination of the weak rotation and the strong magnetic field prior to core collapse makes the explosion energy largest.
2. The toroidal magnetic fields amplified by the field wrapping push the matter outwards as the magnetic pressure and collimate the shock wave near the axis as the hoop stress. On the other hand, the robust explosion near the rotational axis makes the shapes of the shock waves prolate. Thus it is found that the degree of the collimation of the shock waves is determined by the robustness of the asymmetric shock wave and the competition between the hoop stress and the magnetic and the matter pressure.
3. In the models whose initial magnetic fields and initial rotation rates are large, the collimated shock waves are found to carry the strong magnetic fields in the central regions to the outer regions along the rotational axis. In addition, the regions with a relatively low density are found to appear like a nozzle along the rotational axis after the shock wave propagates out of the iron core.
4. Even if the initial poloidal magnetic field is very weak, the strength of the toroidal magnetic field increases with time as a result of the field wrapping over a long rotation periods. As a result, the dynamics in such models is found to be deviated significantly from the pure rotation case.

We should note that there are three major imperfections in our computations. First of all, we did not include the neutrino heating. In addition to the difficulty that hampers us to include it in the multidimensional simulations, we intend here to study the magnetohydrodynamic effects on the explosion mechanism as the first step. The combination of the neutrino heating and the results obtained here will be mentioned in the forthcoming paper (Kotake et al. 2004; Yamada, Kotake, & Yamasaki 2004). Secondly, we assume that the initial magnetic field is just parallel to the rotational axis. This assumption may not be so realistic because the pulsars seem to require the dipole magnetic fields. We are also preparing to treat it as the next step. Finally our simulation does not allow all sorts of MRI. Since our simulations assume axisymmetry that prohibits gradient of vector potential in the toroidal direction, the growth of the poloidal magnetic field due to MRI should be suppressed (Balbus & Hawley 1998). In order to investigate how the MRI contributes to

the amplification of the magnetic field, it is indispensable to perform the three dimensional MHD simulations (e.g. Sano, Inutsuka, Turner, & Stone 2004; Fryer & Warren 2004). In addition it is uncertain whether the number of the grid is enough to resolve the MRI of large wave number. The dependence of the growth rate on the number of grid will be mentioned forthcoming paper.

Bearing these caveats in mind, we state some speculations based on our results. As stated earlier, the models with the strong magnetic fields and the weak rotation initially have the largest explosion energy. It should be noted that the strength of the  $Z$  component of the magnetic fields in the protoneutron star is about  $10^{15}$ G in this model. Thus such model might be related to the formation of the so-called magnetars. It suggests that the explosion accompanied by the formation of the magnetars becomes highly jet-like. However we obtain this result in the initially very strong magnetic field which may seem to be astrophysically unlikely. It should be noted that more systematic parametric search is required. We do not search the initial condition whose  $|T/W|$  is less than 1%. We expect that more slowly rotating core has more robust explosion energy although too slow rotation which prevents the field amplification, should weaken the explosion energy. We have to search more relevant initial condition for magnetar. It should be also mentioned that the regions of low density with the strong toroidal magnetic fields appear along the rotational axis in the models. Since the matter around equatorial plane still falls slowly after the shock waves propagates out of the iron core, there might be another possibility that the highly magnetized protoneutron star collapses to form a black hole in the later time. In the majority of the so-called collapsar models (MacFadyen & Woosley 1999; Proga, MacFadyen, Armitage, & Begelman 2003), the central black hole is assumed to be treated as an initial condition, and then the nozzle near the rotational axis is formed. The nozzle is considered to be the site for producing the gamma-ray bursts. On the other hand, it is expected in our models that the nozzle is likely to be formed before the formation of a black hole. We think that the model, in which the delayed collapse of the protoneutron star to the black hole triggers the gamma-ray bursts (Vietri & Stella 1998), should be also explored by the numerical simulations in context of core-collapse supernovae.

We are grateful to S. Yamada for the fruitful discussions. T. Takiwaki and K. Kotake are also grateful to S. Akiyama for the discussion of MRI. This study was partially supported by Grants-in-Aid for the Scientific Research from the Ministry of Education, Science and Culture of Japan through No.S 14102004, No. 14079202 and No. 16740134.

## REFERENCES

- Akiyama, S., Wheeler, J. C., Meier, D. L., & Lichtenstadt, I. 2003, *ApJ*, 584, 954
- Andersson, N. 2003, *Classical Quantum Gravity*, 20, R105
- Arnett, D. 1996, *Supernovae and Nucleosynthesis* (Princeton: Princeton Univ. Press)
- Balbus, S. A. & Hawley, J. F. 1998, *Reviews of Modern Physics*, 70, 1
- Bisnovatyi-Kogan, G. S. 1971, *Soviet Astron.-AJ*, 14, 652
- Bisnovatyi-Kogan, G. S., & Ruzmaikin, A. A. 1976, *Ap&SS*, 42, 401
- Bodenheimer, P. & Woosley, S. E. 1983, *ApJ*, 269, 281
- Buras, R., Rampp, M., Janka, H.-T., & Kifonidis, K. 2003, *Physical Review Letters*, 90, 241101
- Cropper, M., Bailey, J., McCowage, J., Cannon, R. D., & Couch, W. J. 1988, *MNRAS*, 231, 695
- Duncan, R. C. & Thompson, C. 1992, *ApJ*, 392, L9
- Epstein, R. I. & Pethick, C. J. 1981, *ApJ*, 243, 1003
- Fryer, C. L. & Heger, A. 2000, *ApJ*, 541, 1033
- Fryer, C. L. & Warren, M. S. 2004, *ApJ*, 601, 391
- Heger, A., Langer, N., & Woosley, S. E. 2000, *ApJ*, 528, 368
- Khokhlov, A. M., Höflich, P. A., Oran, E. S., Wheeler, J. C., Wang, L., & Chtchelkanova, A. Y. 1999, *ApJ*, 524, L107
- Kotake, K., Yamada, S., & Sato, K. 2003, *ApJ*, 595, 304
- Kotake, K., Yamada, S., & Sato, K. 2003, *Phys. Rev. D*, 68, 044023
- Kotake, K., Sawai, H., Yamada, S., & Sato, K. 2004, *ApJ* in press
- Kundt, W. 1976, *Nature*, 261, 673
- Leblanc, J. M. & Wilson, J. R. 1970, *ApJ*, 161, 541
- Liebendörfer, M., Mezzacappa, A., & Thielemann, F. 2001, *Phys. Rev. D*, 63, 104003

- Lyutikov, M., Pariev, V. I., & Blandford, R. D. 2003, *ApJ*, 597, 998
- MacFadyen A. I. & Woosley S. E. 1999, *ApJ*, 524, 262
- Meier, D. L., Epstein, R. I., Arnett, W. D., & Schramm, D. N. 1976, *ApJ*, 204, 869
- Mönchmeyer, R. M., & Müller, E. 1989, in *Timing Neutron Stars*, ed. H. Ögelman & E. P. J van den Heuvel (NATO ASI Ser. C, 262; Dordrecht: Kluwer), 549
- Mueller, E. & Hillebrandt, W. 1981, *A&A*, 103, 358
- Nagataki, S., Hashimoto, M., Sato, K., & Yamada, S. 1997, *ApJ*, 486, 1026
- Nagataki, S. 2000, *ApJS*, 127, 141
- Ostriker, J. P. & Gunn, J. E. 1971, *ApJ*, 164, L95
- Papaliolis, C., et al. 1989, *Nature*, 338, 13
- Piran, T. 1999, *Phys. Rep.*, 314, 575
- Plait, P. C., Lundqvist, P., Chevalier, R. A., & Kirshner, R. P. 1995, *ApJ*, 439, 730
- Proga, D., MacFadyen, A. I., Armitage, P. J., & Begelman, M. C. 2003, *ApJ*, 599, L5
- Raffelt, G. G. 2002, in *Proc. Int. School of Physics ee Enrico Fermi, ff CLII Course ee Neutrino Physics ff*
- Rampp, M. & Janka, H.-T. 2000, *ApJ*, 539, L33
- Sano, T., Inutsuka, S., Turner, N. J., & Stone, J. M. 2004, *ApJ*, 605, 321
- Shen, H., Toki, H., Oyamatsu, K. & Sumiyosi, K. 1998 *Nuclear Physics*, A637, 43, 109, 301
- Spruit, H. C. 2002, *A&A*, 381, 923
- Stone, J. M., Mihalas, D., & Norman, M. L. 1992, *ApJS*, 80, 819
- Symbalisty, E. M. D. 1984, *ApJ*, 285, 729
- Tassoul, J. 1978, *Princeton Series in Astrophysics*, Princeton: University Press, 1978,
- Thompson, T. A., Burrows, A., & Pinto, P. A. 2003, *ApJ*, 592, 434
- Vietri, M. & Stella, L. 1998, *ApJ*, 507, L45
- Wang, L., et al. 2002, *ApJ*, 579, 671

Wheeler, J. C., Meier, D. L., & Wilson, J. R. 2002, *ApJ*, 568, 807

Wilson, J. R. 1985, in *Numerical Astrophysics*, ed. J. M. Centrella, J. M. Le Blanc, and R. L. Bowers (Boston: Jones and Barlett), 422

Yamada, S. & Sato, K. 1994, *ApJ*, 434, 268

Yamada, S., Kotake, K., & Yamasaki, T. 2004, submitted to *New. J. Phys.*

Yamada, S. & Sawai, H. 2004, *ApJ* in press

Table 1: Models and Parameters

$B_0$ (Gauss) \ $T/ W $ (%)	1%	2%	4%
0G	B0TW1	B0TW2	B0TW4
$10^9$ G	B9TW1	B9TW2	B9TW4
$10^{10.5}$ G	B10.5TW1	B10.5TW2	B10.5TW4
$10^{12}$ G	B12TW1	B12TW2	B12TW4

---

Note. — This table shows the name of the models. In the table they are labeled by the strength of the initial magnetic field and rotation.  $T/|W|$  represents the ratio of the rotational energy to absolute value of the gravitational energy.  $B_0$  represents the strength of the poloidal magnetic field.

Table 2: Explosion Energy

$B_0$ (Gauss) \ $T/ W $ (%)	1%	2%	4%
0G	0	0	0
$10^9$ G	0.05	0.00077	0
$10^{10.5}$ G	4.7	0.73	0.03
$10^{12}$ G	44	5.6	1.8

---

Note. — The explosion energy for each model is given. For the definition of the explosion energy, see Eq. (8). It's noted that they are normalized as  $10^{50}$ erg.

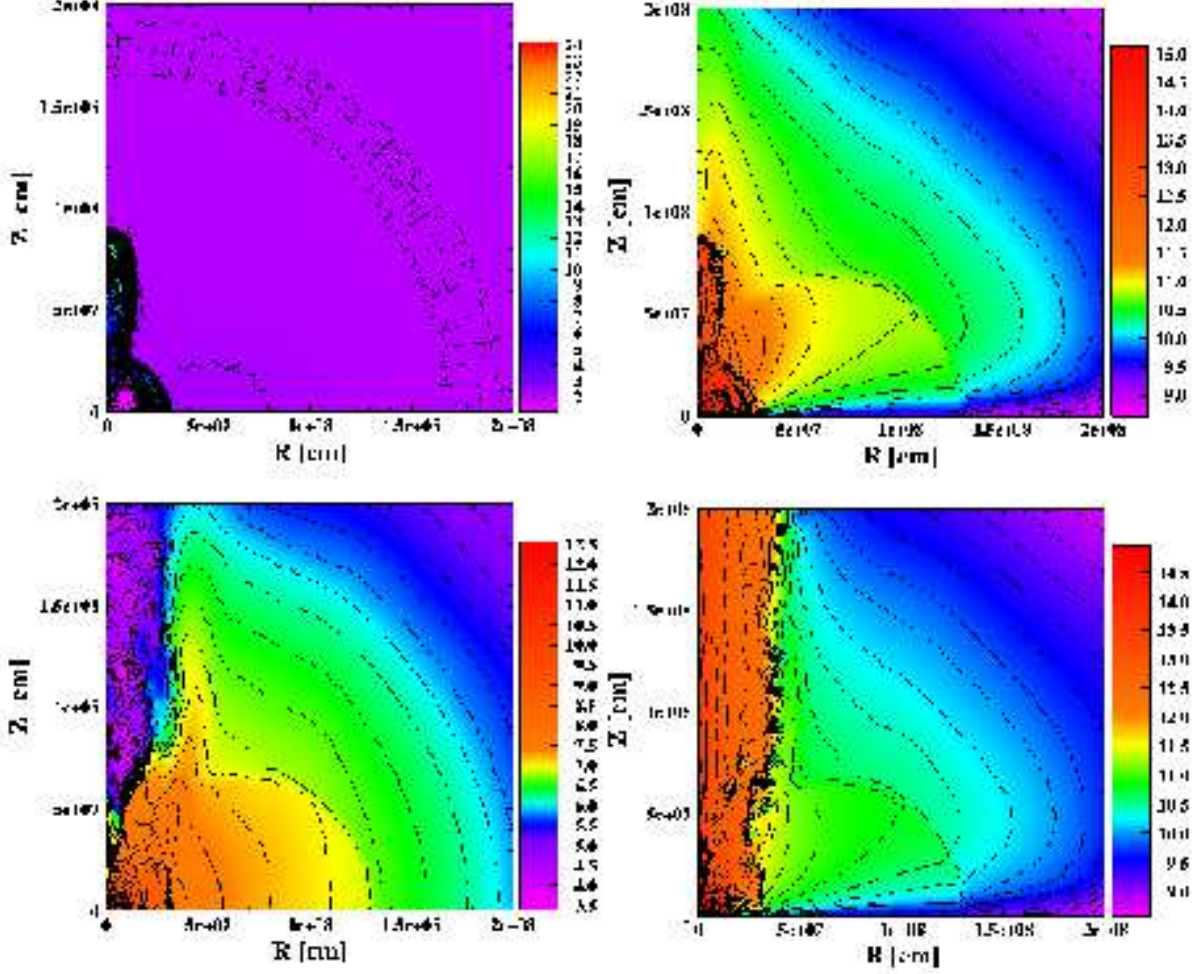


Fig. 1.— Various profiles of model B12TW4. Each figure shows entropy per nucleon at  $t = 32$ ms (from core bounce) (left top), the logarithm of toroidal magnetic field (G) at  $t = 32$ ms (right top), the logarithm of density ( $\text{g}/\text{cm}^3$ ) at  $t = 57$ ms (left bottom) and the logarithm of toroidal magnetic field (G) at  $t = 57$ ms (right bottom). The top figures show that the magnetic field becomes strong behind the shock wave. The bottom figures show the properties after propagation of the shock wave. In the left figure, It's found that a nozzle is formed near the rotational axis, where the density is significantly lowered.

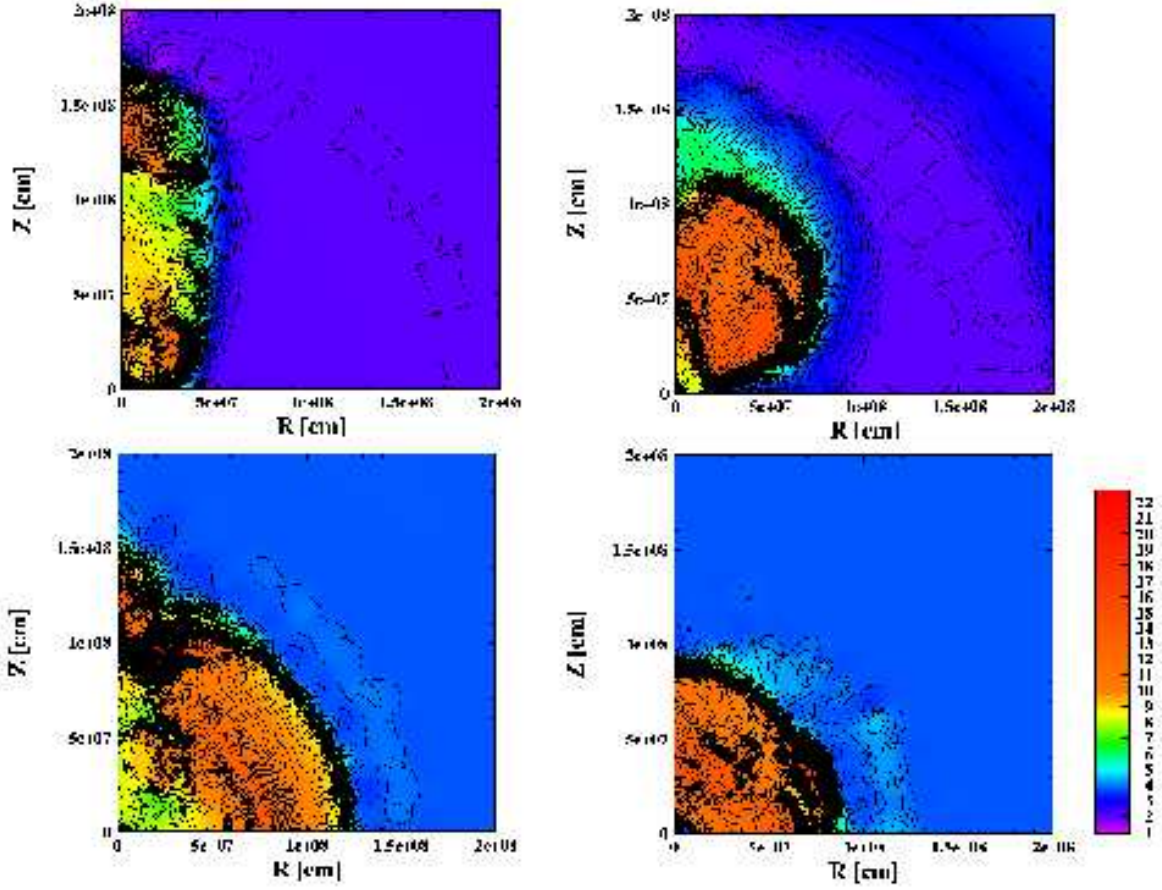


Fig. 2.— Profiles of the shock propagation in the various models. Each panel demonstrates B12TW2 at 60ms from core bounce (top left), B10.5TW1 at 127ms (top right), B10.5TW2 at 219ms (bottom left), B9TW4 at 404ms (bottom right). They show the color coded contour plots of entropy ( $k_B$ ) per nucleon. Various profiles are found by changing the strength of the initial magnetic field and rotation.

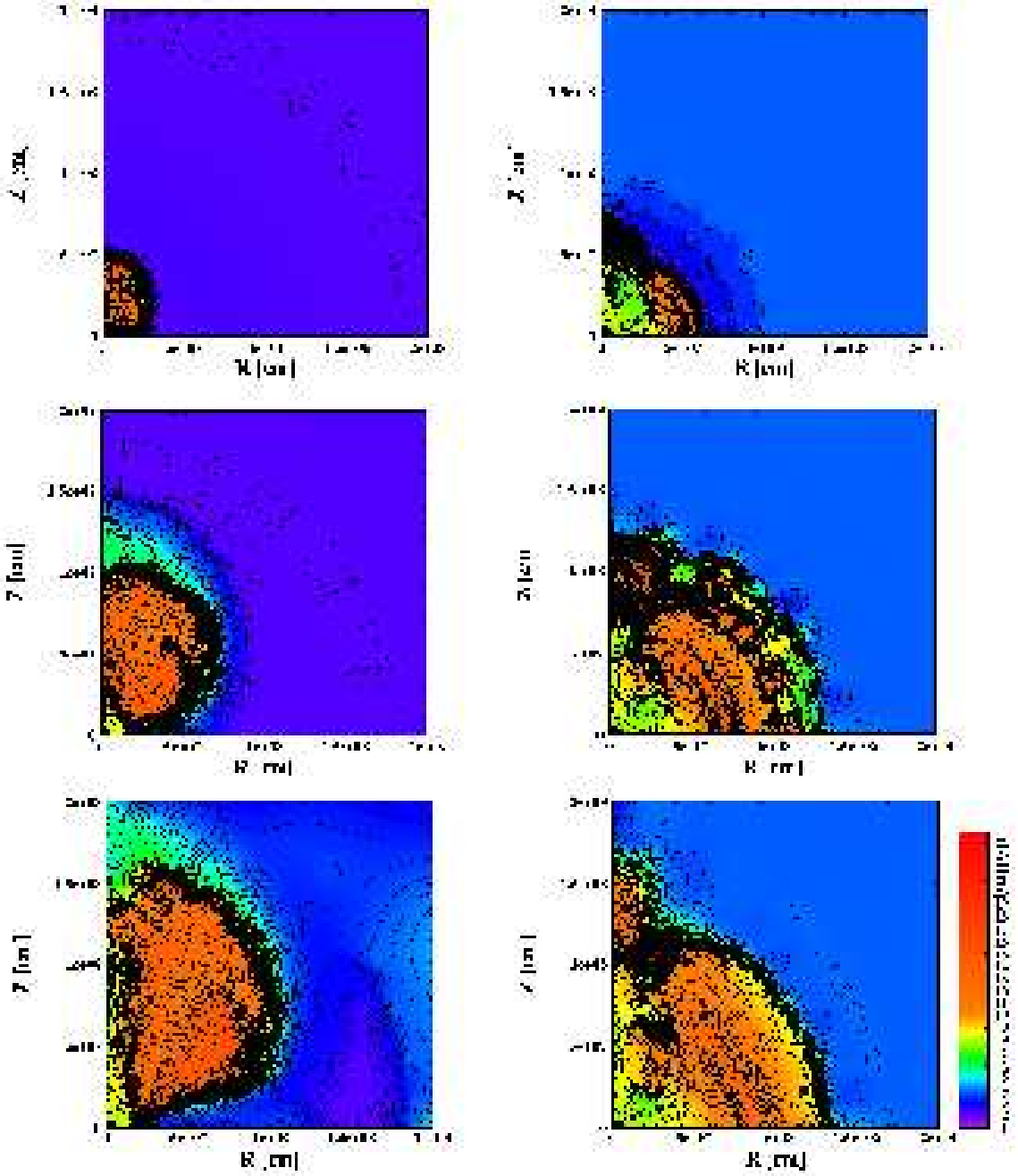


Fig. 3.— Time evolution of shock waves for B10.5TW1 and B10.5TW2. These figures show color coded contour plots of entropy ( $k_B$ ) per nucleon. The three figures at the left side correspond to the model B10.5TW1, at  $t = 52\text{ms}$ ,  $127\text{ms}$ ,  $219\text{ms}$  from top to bottom, respectively. The three figures at the right side correspond to the model B10.5TW2, at  $t = 355\text{ms}$ ,  $405\text{ms}$ ,  $430\text{ms}$  from top to bottom. We discuss the features of this evolution in subsection 3.1.

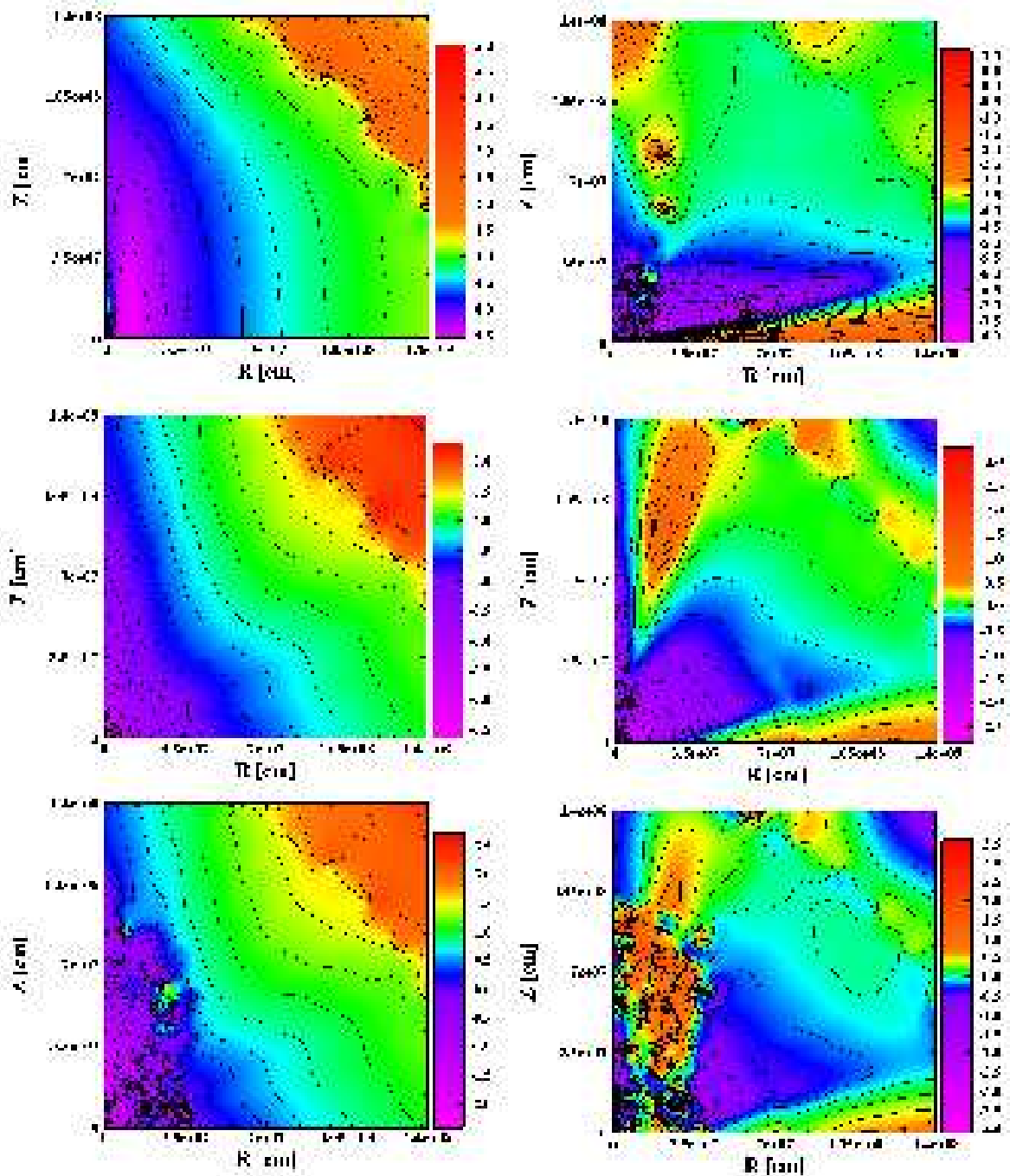


Fig. 4.— The characteristic time scale of the maximum growth of the MRI and the variation of the toroidal magnetic field. This figure shows the contour of the logarithm of the  $\tau_{\text{MRI}}$  [s] (left) and the counter of the logarithm of the  $\tau_{\text{WRAP}}$  [s] (right) in the model of B12TW2. The top figures show two time-scales at the onset of core collapse ( $-172\text{ms}$  from core bounce), the middle figures show these at near the core bounce ( $5\text{ms}$ ), the bottom figures show these when jet propagates ( $25\text{ms}$ ).

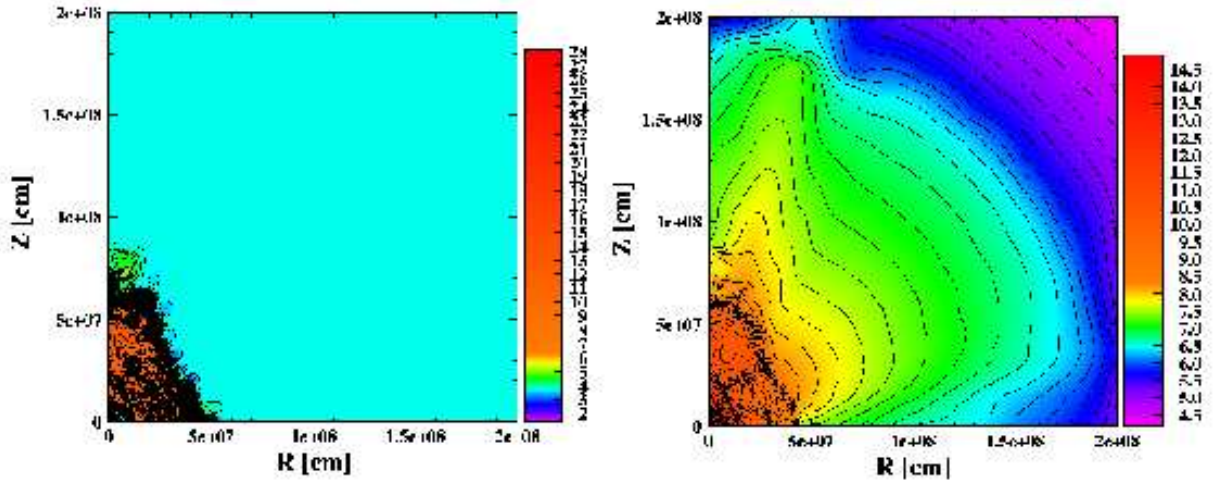


Fig. 5.— This figure shows entropy (left) and logarithm of the toroidal magnetic field (right) of model B9TW4. Small jet is generated by the magnetic pressure. The model B9TW4 begin with the weak magnetic field, however we found the weak jet at the later stage (366ms from core bounce). The toroidal magnetic field has been sufficiently amplified by the differential rotation in the later stage.

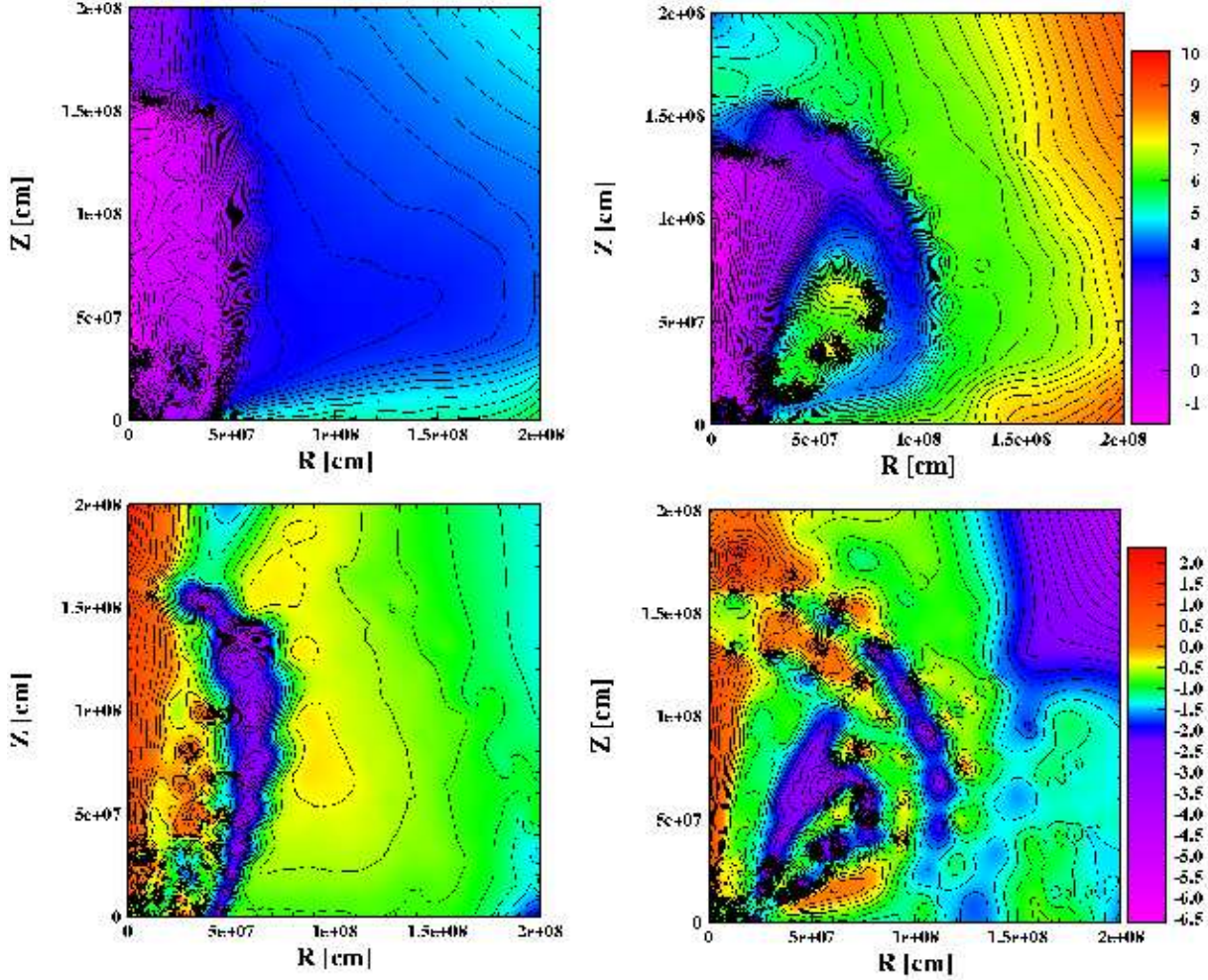


Fig. 6.— The top panel of the figure shows logarithm of the plasma beta of model B10.5TW1 (right, 243ms from core bounce) and model B12TW2 (left, 60ms from core bounce). If  $\beta < 1$  inside the shock wave, the jet is collimated. On the other hand, if there is region with  $\beta > 1$  inside the jet, the shape of the jet becomes less collimated. The bottom panel of figure the figure shows logarithm of the ratio of the hoop stress to the magnetic pressure. This figure demonstrates clearly that the shock wave is collimated by the hoop stress near the rotational axis.